ACS Pharmacology & Translational Science

pubs.acs.org/ptsci Article

A New Selective Pharmacological Enhancer of the Orai1 Ca^{2+} Channel Reveals Roles for Orai1 in Smooth and Skeletal Muscle Functions

Iman Azimi, Ralph J. Stevenson, Xuexin Zhang, Aldo Meizoso-Huesca, Ping Xin, Martin Johnson, Jack U. Flanagan, Silke B. Chalmers, Ryan E. Yoast, Jeevak S. Kapure, Benjamin P. Ross, Irina Vetter, Mark R. Ashton, Bradley S. Launikonis, William A. Denny, Mohamed Trebak,*, and Gregory R. Monteith*,

Cite This: *ACS Pharmacol. Transl. Sci.* 2020, 3, 135−147 Read Online

ACCESS | Metrics & More | Article Recommendations | Supporting Information

ABSTRACT: Store-operated calcium (Ca^{2+}) entry is an important homeostatic mechanism in cells, whereby the release of Ca^{2+} from intracellular endoplasmic reticulum stores triggers the activation of a Ca^{2+} influx pathway. Mediated by Orai1, this Ca^{2+} influx has specific and essential roles in biological processes as diverse as lactation to immunity. Although pharmacological inhibitors of this Ca^{2+} influx mechanism have helped to define the role of store-operated Ca^{2+} entry in many cellular events, the lack of isoform specific modulators and activators of Orai1 has limited our full understanding of these processes. Here we report the identification and synthesis of an Orai1 activity enhancer that concurrently potentiated Orai1 Ca^{2+}-dependent inactivation (CDI). This unique enhancer of Orai1 had only a modest effect on Orai3 with weak inhibitory effects at high concentrations in intact MCF-7 breast cancer cells. The Orai1 enhancer heightened vascular smooth muscle cell migration induced by platelet-derived growth factor and the unique store-operated Ca^{2+} entry pathway present in skeletal muscle cells. These studies show that IA65 is an exemplar for the translation and development of Orai isoform selective agents. The ability of IA65 to activate CDI demonstrates that agents can be developed that can enhance Orai1-mediated Ca^{2+} influx but avoid the cytotoxicity associated with sustained Orai1 activation. IA65 and/or future analogues with similar Orai1- and CDI-activating properties could function to fine-tune physiological processes important in specific disease states, such as cellular migration and immune cell function.

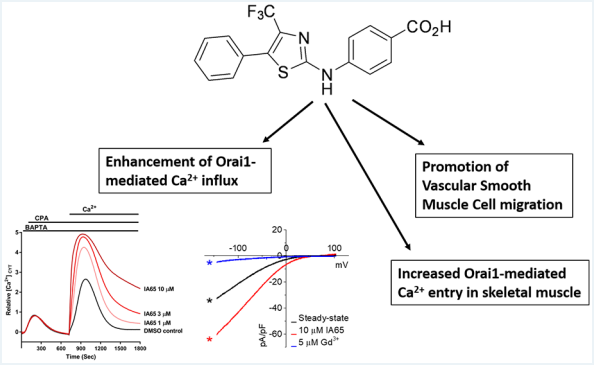

KEYWORDS: *Orai1, Ca^{2+} influx, enhancer, smooth muscle, skeletal muscle*

Release of Ca^{2+} from the endoplasmic reticulum (ER) is a key event in cellular signaling pathways involving activation of many G-protein coupled and tyrosine kinase receptors. Activation of phospholipase C by these receptors results in inositol 1,4,5-trisphosphate (IP_3) generation and depletion of ER Ca^{2+} stores.[1] Calcium-release-activated calcium (CRAC) channels, which are made up of hexamers of the protein Orai1, are responsible for the influx of Ca^{2+} after receptor-mediated depletion of ER Ca^{2+} stores.[2−4] This canonical pathway is termed store-operated Ca^{2+} entry (SOCE) and involves the activation of Orai1 channels by the ER Ca^{2+} store sensor STIM1.[5−7]

The consequence of the absence or loss of function of Orai1 is manifested in humans by a severe combined immune-deficiency (SCID)-like condition, autoimmunity, anhidrosis (inability to sweat normally), tooth enamel defects, and generalized muscle weakness.[5,8] A variety of studies have now provided clear mechanistic insights into the critical role for Orai1-mediated Ca^{2+} influx in a variety of physiological processes as diverse as T-cell mediated immunity, lactation, and gene transcription.[9−11] The aberrant expression or activity of Orai1 in disease models has seen pharmacological modulators of CRAC currently postulated as therapies for a diverse set of conditions such as inflammatory bowel disease, asthma, psoriasis, and cancer.[12,13] Indeed, assessment of pharmacological inhibitors of CRAC in mouse *in vivo* models has shown their ability to protect against acute pancreatitis[14] and breast cancer metastasis.[15] The commencement of clinical

Received: October 12, 2019
Published: January 13, 2020

https://dx.doi.org/10.1021/acsptsci.9b00081
ACS Pharmacol. Transl. Sci. 2020, 3, 135−147

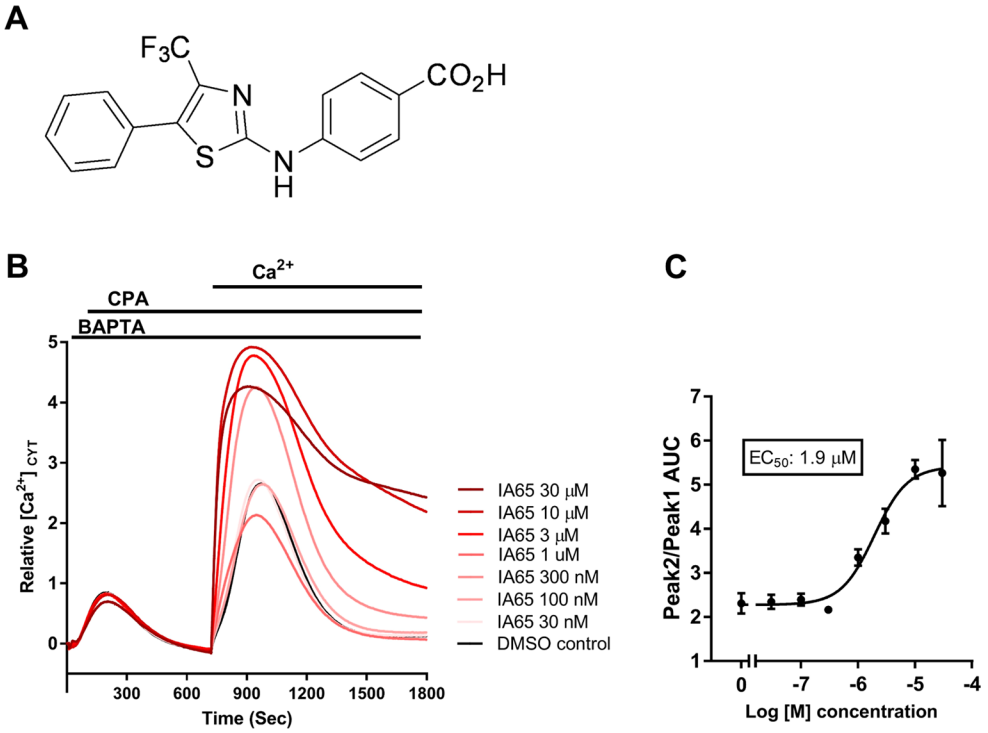

Figure 1. IA65 promotes Orai1-mediated Ca^{2+} influx. (A) Chemical structure of IA65. (B) Mean $[Ca^{2+}]_{CYT}$ levels during assessment of SOCE in MDA-MB-231 cells treated with increasing concentrations of IA65. Cells were pretreated with IA65 for 15 min at room temperature, and IA65 concentrations were maintained during an assessment of SOCE. (C) Intracellular Ca^{2+} measurements as area under curve (AUC) calculated during SOCE Ca^{2+} influx, after treatment of cells with vehicle control or increasing concentrations of IA65 (30 nM to 30 μM) in MDA-MB-231 cells. n = 3, mean ± SD.

trials of CRAC inhibitors for acute pancreatitis, relapsed or refractory non-Hodgkin's lymphoma, and psoriasis are reflective of the pharmacotherapy opportunities for this class of agents.[12]

Our full understanding of Orai1, however, has been limited by the delay in the development of pharmacological activators of Orai1-mediated Ca^{2+} influx. Pharmacological activators have proven to be powerful tools to define the role of other Ca^{2+}-permeable ion channels in cellular processes and as potential therapeutic targets. Such agents include activators of TRPV1 (capsaicin), TRPV4 (GSK1016790A) and L-type Ca^{2+} channels ((*S*)-(−)-BAY K 8644). Although Orai3 but not Orai1 can be activated by 50 μM 2-aminoethyldiphenyl borinate (2-APB),[16] 2-APB is a largely nonselective tool that has been shown to affect a plethora of ion channels with distinct structures and subcellular locations.[17] Thus, pharmacological tools necessary to fully probe the consequences of Orai1 activation are currently lacking. Given the coexpression of Orai isoforms in many cell types, such as in MCF-7 breast cancer cells where both Orai1 and Orai3 can function as store-operated Ca^{2+} channels,[18] some selectivity for Orai1 over Orai3 is critical. Sustained pharmacological activation of Orai1 may be detrimental, given that Orai1 gain of function mutations result in muscle cramping, muscle stiffness, limited joint movement, persistent pupil constriction, ichthyosis (dry, thick, and scaly skin), and dyslexia[19] and because of the role of Orai1 in cell death associated with acute pancreatitis.[14] Hence, compounds that enhance Orai1 activity triggered by store depletion while concomitantly promoting Orai1 calcium-dependent inactivation (CDI)[20] and exhibiting some selectivity over Orai3 may allow promotion of near-physiological Orai1-mediated Ca^{2+} entry during key events without either inducing cytotoxicity from Ca^{2+} overload or triggering Orai3-dependent pathways. CDI has been recently shown to be critical in defining the nature of cytosolic free Ca^{2+} ($[Ca^{2+}]_{CYT}$) transients and the regulation of the Ca^{2+}-dependent transcription factor nuclear factor of activated T-cells (NFAT).[21] Riva et al.[22] very recently reported a family of pyrtriazoles that included agents that act as SOCE inhibitors or activators or enhancers; however, activation effects were modest and Orai3 selectivity and effects on CDI were not defined.

Here, we identify and characterize a new pharmacological tool for the selective enhancement of Orai1-mediated Ca^{2+} influx. This agent, which we termed IA65, enhances Orai1 activity with concurrent enhancement of Orai1 CDI and little effect on Orai3. We use this new tool to provide new insights into the role of Orai1 in smooth and skeletal muscles.

RESULTS

During an assessment of a library of over 2100 small-molecule compounds from ChemBridge as potential inhibitors of SOCE in MDA-MB-231 breast cancer cells, where SOCE is mediated by Orai1,[23,24] one benzoic acid was identified as a promotor of SOCE. 4-((5-Phenyl-4-(trifluoromethyl)thiazol-2-yl)amino)-benzoic acid (IA65, Figure 1A) had no effect on the Ca^{2+} release from ER Ca^{2+} stores via the sarco-/ER Ca^{2+}-ATPase (SERCA) inhibitor cyclopiazonic acid (CPA). However, unlike previously described modulators of SOCE,[24−26] IA65 augmented rather than inhibited the Ca^{2+} influx induced by ER Ca^{2+} store depletion with an EC_{50} of ∼1.9 μM (Figure 1B,C). Analogues of IA65 exhibit either more modest (e.g., 19) or no promotion (e.g., 1) or even modest inhibition (e.g., 17) of SOCE (Table S1). IA65 did not show any activity (neither inhibition nor activation) against TRPV1, TRPM8, or $Ca_V2.2$

https://dx.doi.org/10.1021/acsptsci.9b00081
ACS Pharmacol. Transl. Sci. 2020, 3, 135−147

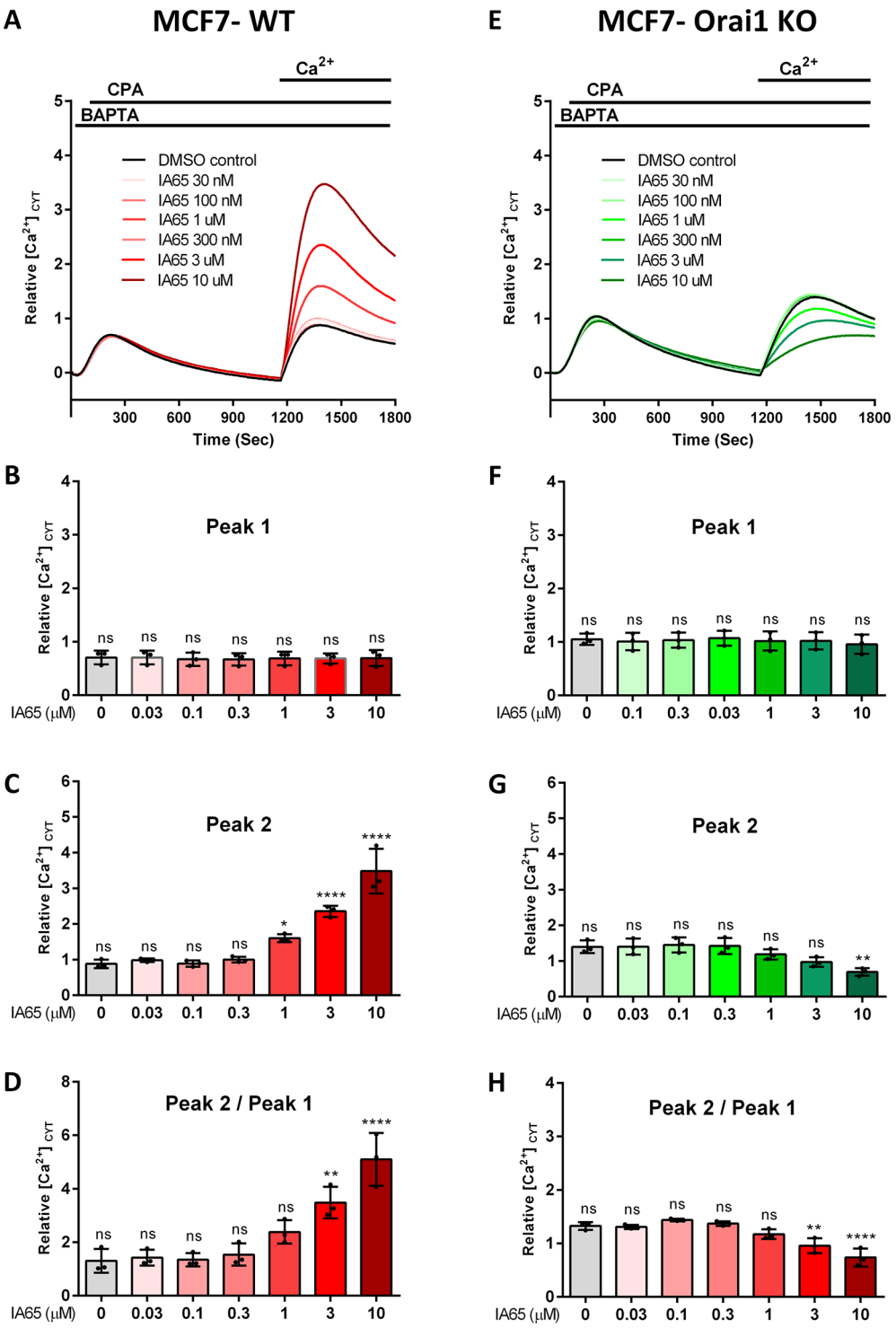

Figure 2. IA65 activates native Orai1, but not Orai3-mediated SOCE in MCF-7 cells. Mean $[Ca^{2+}]_{CYT}$ levels and quantitative analysis during assessment of SOCE in (A–D) MCF7-WT and (E–H) MCF7-Orai1 KO cells. Cells were pretreated with IA65 for 15 min at room temperature and IA65 concentrations were maintained during assessment of SOCE. ns = not significant ($p > 0.05$); *, $p < 0.05$; **, $p < 0.01$; and ****, $p < 0.0001$ (one-way ANOVA, with Dunnett's multiple comparisons). $n = 3$, mean ± SD.

at concentrations up to 100 μM (Table S2). IA65 also did not cause any toxicity in MDA-MB-231 cells at concentrations up to 100 μM (Figure S1).

To define the mechanisms of IA65 action on SOCE, we exploited the phenomena in estrogen-receptor-positive MCF-7 breast cancer cells whereby SOCE is mediated by both Orai1 and Orai3.[18] Consistent with results in MDA-MB-231 breast cancer cells, in wild type MCF-7 breast cancer cells, IA65 promoted SOCE with significant augmentation of Ca^{2+} influx at 1 μM with no effects on Ca^{2+} release induced by CPA at any assessed concentration (Figure 2A–D). In contrast, in MCF-7 cells with CRISPR-mediated knockout of Orai1 (Orai1 KO), no promotion of SOCE was observed at any concertation of IA65 assessed (Figure 2E–H). Instead, IA65 significantly

https://dx.doi.org/10.1021/acsptsci.9b00081
ACS Pharmacol. Transl. Sci. 2020, 3, 135–147

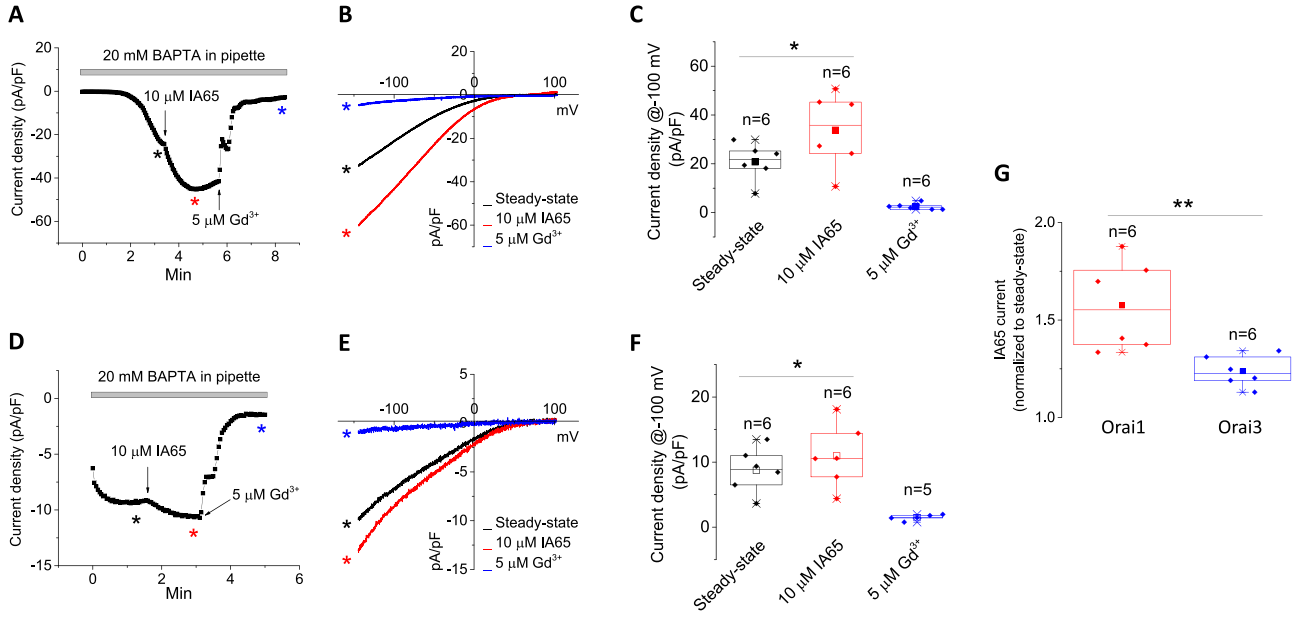

Figure 3. IA65 enhanced Orai1 I_{CRAC}. (A) Whole-cell patch clamp recording in Orai1/2/3 triple-knockout HEK293 cells expressing STIM1 along with Orai1 shows that Orai1-mediated CRAC current is enhanced by 10 μM IA65 and blocked by 5 μM Gd^{3+}. (B) Representative $I-V$ curves on current traces taken where indicated by the color-coded asterisks. (C) Current densities. (D) Whole-cell patch clamp recording in Orai1/2/3 triple-knockout HEK293 cells coexpressing STIM1 and Orai3 shows that Orai3-mediated CRAC current are not as affected by application of 10 μM IA65, but are blocked by 5 μM Gd^{3+}, as expected. (E) Representative $I-V$ relationships. (F) Current densities. (G) Comparison of the magnitude of enhancement of Orai1 and Orai3 CRAC currents by IA65 shows significantly greater enhancement of Orai1 compared to Orai3. Data were statistically analyzed using a paired sample t test and represented as mean ± SEM (*, $p < 0.05$; **, $p < 0.01$). Pair-sample t-test was used for panels C and F; two-sample t-test was used for panel G.

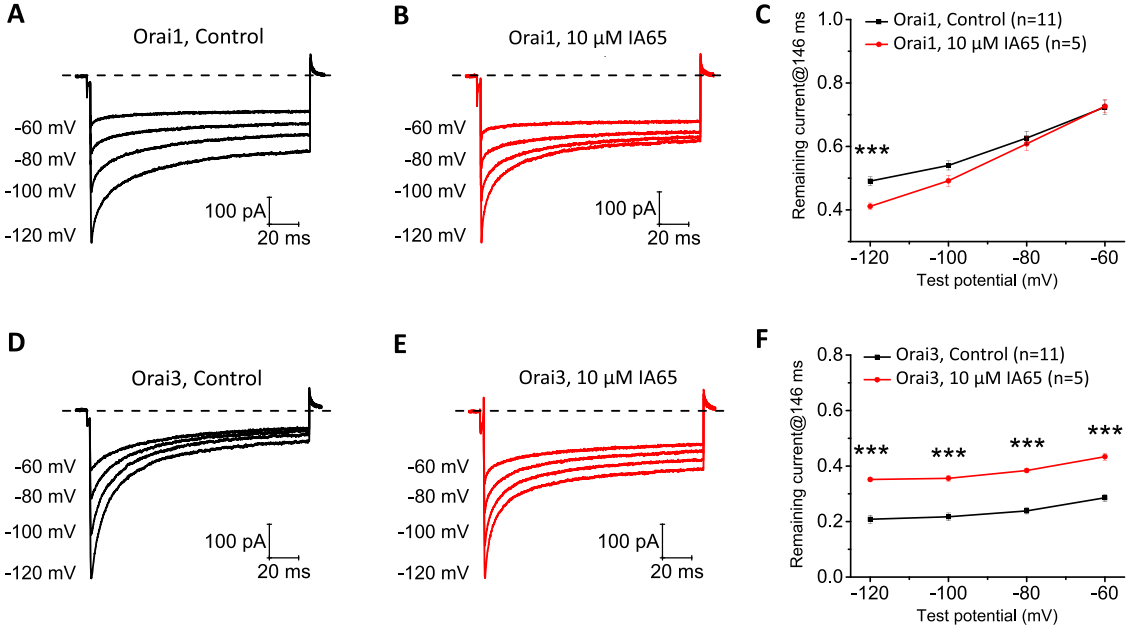

Figure 4. Effect of IA65 on CDI from Orai1 and Orai3 channels. Representative currents were recorded from Orai1/2/3 triple-knockout HEK293 cells coexpressing STIM1 and Orai1. EGTA (10 mM) in the patch pipet was used to cause store depletion, and I_{CRAC} was recorded in the presence of either (A) vehicle control or (B) IA65 at 10 μM in the bath solution. (C) For quantification of CDI, the extent of inactivation at 146 ms, the residual current remaining at the end of the test pulse (at 146 ms) relative to the peak current at 3 ms was plotted against test potential. (D and E) Representative currents assessing CDI under the same protocol were recorded from Orai1/2/3 triple-knockout HEK293 cells coexpressing STIM1 and Orai3. (F) For quantification of CDI, the extent of inactivation at 146 ms, the residual current remaining at the end of the test pulse (at 146 ms) relative to the peak current at 3 ms was plotted against test potential. ***, $p < 0.001$; two-tailed Student's t test was used for panels C and F.

reduced SOCE at the higher concentrations of 3 and 10 μM in MCF-7 Orai1 KO cells, suggesting a possible effect on Orai3 under these conditions, given that Orai3 mediates SOCE in MCF-7 cells. The protocols and guide RNAs used for Orai1 knockout in MCF7 cells are listed in the Materials and Methods. Orai1 knockdown in MCF7 cells was documented

https://dx.doi.org/10.1021/acsptsci.9b00081
ACS Pharmacol. Transl. Sci. 2020, 3, 135−147

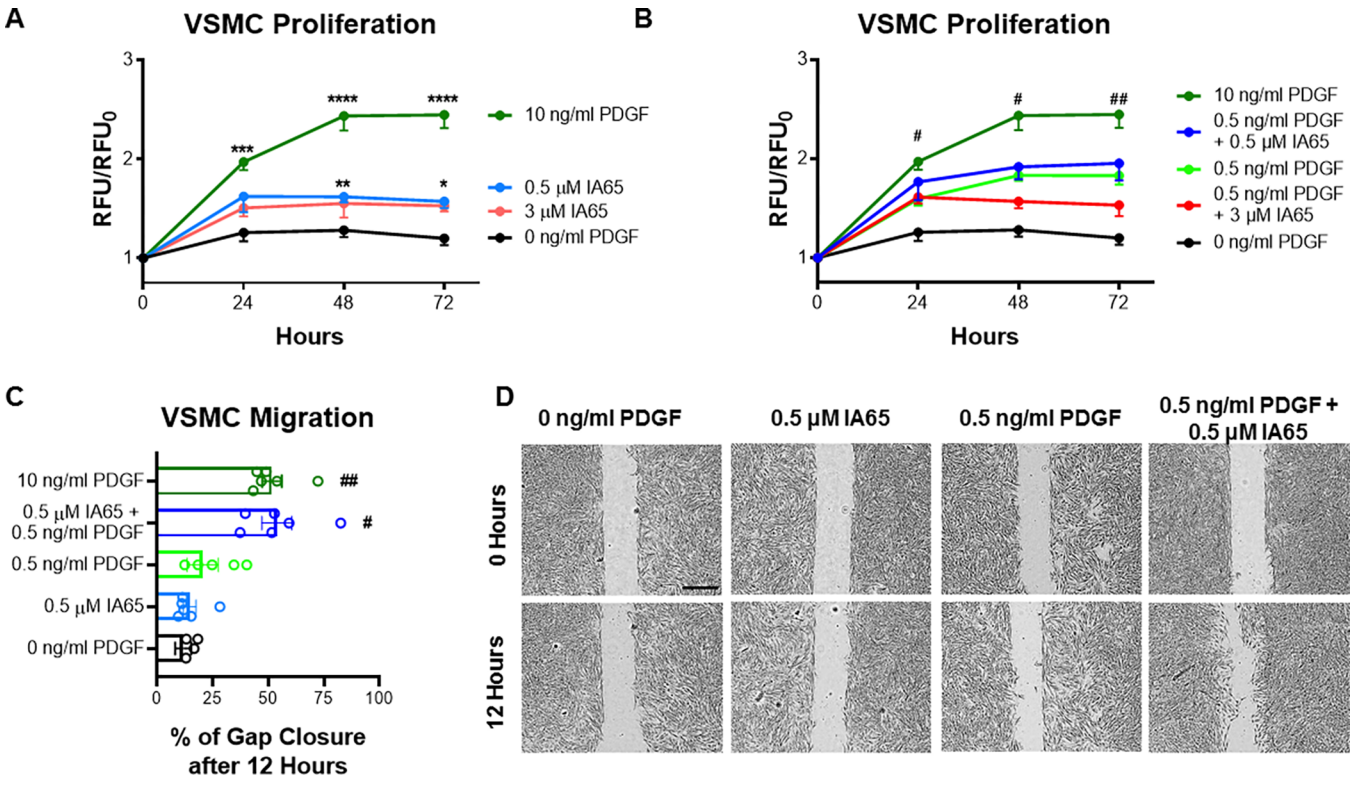

Figure 5. IA65 promotes vascular smooth muscle cell (VSMC) migration. (A) VSMC showed significant proliferation in response to IA65 (0.5 and 3 μM) at 48 and 72 h compared to 0 ng/mL PDGF control. Maximal concentrations of PDGF (10 ng/mL) were used as a positive control. (B) Both 0.5 and 3 μM IA65 did not synergize with low concentrations of PDGF (0.5 ng/mL) in VSMC proliferation. (C) A dose of 0.5 μM IA65 did not induce significant VSMC migration at 12 h but showed a synergistic effect on VSMC migration when added with a low concentration of PDGF (0.5 ng/mL), comparable to maximal concentrations of PDGF (10 ng/mL). (D) Representative bright-field images of gap-closure experiments. Scale bar equals 500 μm. ANOVA and Dunnett's multiple comparison test were used for proliferation and migration experiments. *, $p < 0.05$; **, $p < 0.01$; ***, $p < 0.001$; and ****, $p < 0.0001$ when compared to 0 ng/mL of PDGF. #, $p < 0.05$, and ##, $p < 0.01$, when compared to 0.5 ng/mL of PDGF.

by genome sequencing and by Western blotting using an Orai1-specific antibody (Figure S2).

To directly assess the effect of IA65 on Orai1-mediated CRAC currents (I_{CRAC}), I_{CRAC} recordings in HEK293 cells coexpressing STIM1 with either Orai1 or Orai3 using the weaker more physiological chelator EGTA to deplete stores were conducted. This showed that preincubation of cells with IA65 at either 3 or 10 μM caused concentration-dependent potentiation of Orai1-mediated currents with no effect on Orai3-mediated currents (Figures S3 and S4), consistent with SOCE effects in intact MCF-7 breast cancer cell lines (Figure 2).

We then assessed the effect of IA65 on Orai1 and Orai3 coexpressed with their protein activator, the ER Ca^{2+} sensor STIM1, in HEK293 cells lacking all three Orai isoforms (Orai triple-knockout; Orai-TKO). Protocols and specific guide RNAs (gRNAs) used for the generation of Orai-TKO cells are listed in the Materials and Methods. We used two independent gRNA flanking each Orai gene to completely excise the gene, allowing us to use the total loss of mRNA (as assessed by RT-qPCR) as a reliable means for documenting knockout. The use of this strategy is critical for knockout of Orai2 and Orai3, for which no reliable antibodies currently exist. In addition to genome sequencing, RT-qPCR for Orai2 and Orai3 isoforms and Western blots for Orai1 were used to document knockout (Figure S5). In these recordings, we used 20 mM of the fast buffer BAPTA to deplete the ER Ca^{2+} stores while preventing Ca^{2+}-dependent inhibition (CDI) of Orai channels driven by rises in $[Ca^{2+}]_{CYT}$. Under these conditions, 10 μM IA65 enhanced I_{CRAC} mediated by Orai1 (Figure 3A–C). This enhancement of Orai1 I_{CRAC} by IA65 was abolished by the I_{CRAC} inhibitor gadolinium (Gd^{3+}) at the low concentration of 5 μM (Figure 3A–C). Despite strong cytosolic Ca^{2+} buffering with BAPTA to abrogate CDI, I_{CRAC} measurements using the same protocol in Orai-TKO HEK293 cells coexpressing Orai3 and STIM1 showed only slight potentiation of Orai3 I_{CRAC} by IA65, providing further evidence that IA65 (10 μM) is only a marginal Orai3 regulator under highly permissive "non-physiological" conditions (Figure 3D–F). Indeed, the enhancement of Orai1 was significantly greater than for Orai3 (Figure 3G). Further assessment also identified that IA65 had a unique ability to also enhance Orai1 but not Orai3 CDI (which was inhibited) (Figure 4A–F), suggesting that it may be possible to fine-tune Orai1-mediated Ca^{2+} signaling and avoid the deleterious effects of sustained Orai1 activation.

We then performed concentration–response analysis of IA65 (at 1, 3, and 10 μM) on CDI of Orai1 and Orai3 coexpressed with STIM in Orai-TKO HEK293 cells using 10 mM EGTA in the patch pipet. The results depicted in Figure S6 show that IA65 enhanced CDI of Orai1 in a concentration-dependent manner while inhibiting CDI of Orai3. Similar recordings of Orai1 CDI in Orai-TKO cells coexpressing Orai1 and STIM1 and using 20 mM of the strong buffer BAPTA in

https://dx.doi.org/10.1021/acsptsci.9b00081
ACS Pharmacol. Transl. Sci. 2020, 3, 135–147

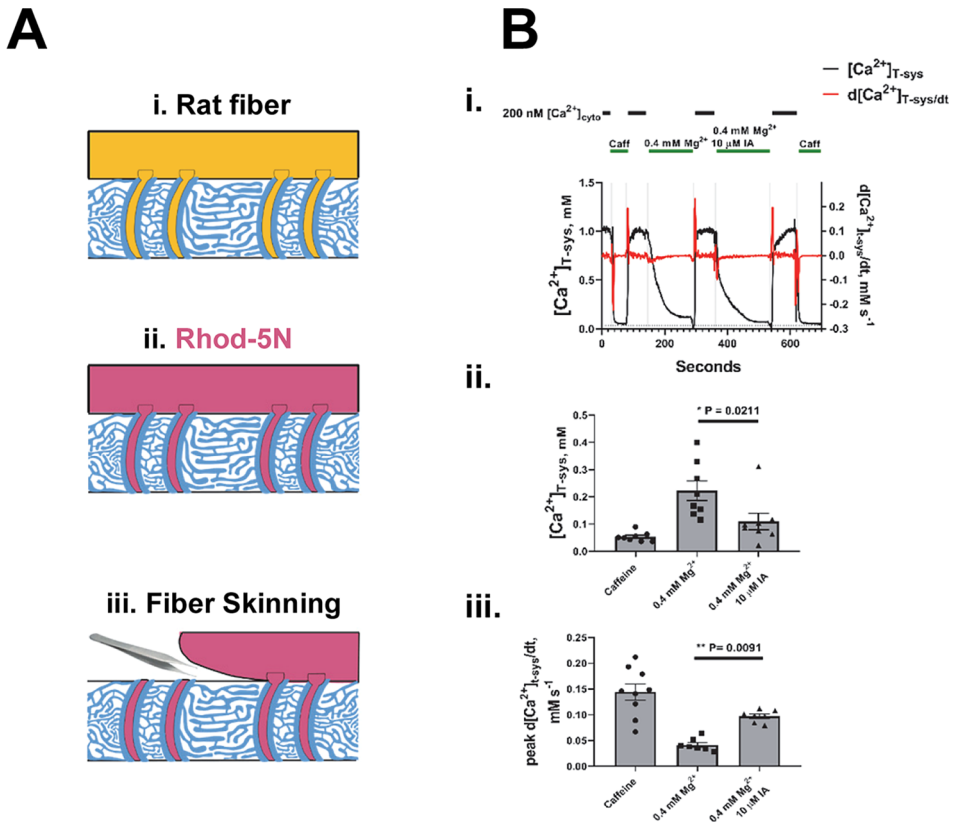

Figure 6. Effect of IA65 on t-system calcium movements. Schematic representation of the steps of loading dye into the t-system, to track $[Ca^{2+}]_{t\text{-}sys}$ transients. (A) Intact rat fiber in standard physiological solution (yellow). (B) A physiological solution containing rhod-5N (red) is introduced to the intact fiber, allowing the dye to diffuse into the t-system. (C) The fiber is mechanically skinned with fine forceps, which causes the t-system to seal at the former interface between the outer plasma membrane and the t-system and trap the dye in the extracellular space (t-system). (D) Spatially averaged t-system Rhod-5N signal during a series of solution exchanges from resting solution, where $[Ca^{2+}]_{t\text{-}sys}$ reaches a steady state in the mM range, to fully (caffeine 30 mM, Ca^{2+} 0 mM, Mg^{2+} 0.01 mM) or partially (Ca^{2+} 0 mM, Mg^{2+} 0.4 mM with and without 10 μM IA65) activate SOCE (shown in black). The t-system Ca^{2+} flux was derived from $[Ca^{2+}]_{t\text{-}sys}$ (shown in red). (E) The t-system Ca^{2+} concentration after the different Orai1 activation conditions. (F) Peak t-system Ca^{2+}efflux induced by the different Orai1 activation conditions. Data was compared by one-way ANOVA with Tukey's post hoc test (*, $p < 0.05$). $N = 6-8$.

the patch pipet to elicit I_{CRAC} clearly showed that IA65 enhancement of Orai1 CDI is maintained in the presence of BAPTA, suggesting that the effect of IA65 is at least partially Ca^{2+}-independent (Figure S7). Indeed, we performed similar Orai1 CDI recordings on the same cells and under the same intracellular buffering conditions, except that 20 mM extracellular Ca^{2+} was now substituted with 20 mM Ba^{2+}. In the presence of 20 mM extracellular Ba^{2+}, Orai1 CDI was apparent only when IA65 was added to the bath solution and the tail current was reduced, a strong argument for the effect of IA65 on Orai1 CDI being at least partially Ca^{2+}-independent (Figure S8).

The evaluation of the physiological consequences of Orai1-mediated Ca^{2+} influx enhancement and promotion of CDI was assessed in the context of vascular smooth muscle cell (VSMC) proliferation and migration. As expected, the maximal concentration of the platelet-derived growth factor (PDGF; 10 ng/mL) produced a pronounced stimulation of proliferation with low concentrations of IA65 (0.5 or 3 μM) producing only a modest effect (Figure 5A). Furthermore, IA65 did not enhance the pro-proliferative effects of a submaximal concentration of PDGF (0.5 ng/mL) (Figure 5B), suggesting that the effects of submaximal concentrations of IA65 and PDGF on VSMC proliferation are not additive. In contrast, consistent with the reported role of Orai1 in migration in a variety of cell types,[27−31] IA65 significantly enhanced the ability of submaximal concentrations of PDGF to enhance the migration of VSMCs (Figure 5C,D). The ability of IA65 to augment rather than suppress migration of VSMCs was also consistent with a lack of cytotoxicity of IA65 at concentrations that promoted SOCE (Figure S1).

To assess the effect of IA65 on Orai1-mediated Ca^{2+} entry in skeletal muscle, mechanically skinned fibers from rat extensor digitorum longus (EDL) muscles were used. A Ca^{2+}-sensitive dye (rhod-5N) was trapped in the tubular (t-)system and used to monitor Ca^{2+} movements across the t-system membrane.[32] By tracking the t-system $[Ca^{2+}]$ ($[Ca^{2+}]_{t\text{-}sys}$) transient, SOCE activity and thus Orai1 activity can be tracked (Figure 6A−C). The experiment in Figure 6D shows $[Ca^{2+}]_{t\text{-}sys}$ transient initially in the presence of a resting cytoplasmic solution with 200 nM $[Ca^{2+}]_{cyto}$. In this solution the $[Ca^{2+}]_{t\text{-}sys}$ displays a steady level of around 1 mM. The substitution of this solution for 30 mM caffeine in the presence of 0.01 mM $[Mg^{2+}]_{cyto}$ causes a rapid release of Ca^{2+} from the sarcoplasmic reticulum (SR) and a rapid activation of SOCE and a depletion of $[Ca^{2+}]_{t\text{-}sys}$ to approximately 0.05 mM.[32−36] Exchange of the caffeine solution for the resting solution with 200 nM $[Ca^{2+}]_{cyto}$ allows the $[Ca^{2+}]_{t\text{-}sys}$ to reach mM levels again. From the same $[Ca^{2+}]_{t\text{-}sys}$ (and therefore the same driving force for Ca^{2+} entry, DF_{Ca}), the effect of a solution containing 0.4

https://dx.doi.org/10.1021/acsptsci.9b00081
ACS Pharmacol. Transl. Sci. 2020, 3, 135−147

mM $[Mg^{2+}]_{cyto}$ and no added Ca^{2+} was applied to observe the effect of a submaximal increases in the activity of the ryanodine receptor (RyR) on the rate of Orai1-dependent Ca^{2+} entry. In this solution, the $[Ca^{2+}]_{t\text{-}sys}$ transient declined, but more slowly than it did in the presence of caffeine. Note that caffeine and low $[Mg^{2+}]_{cyto}$ activate the RyR without changing the resting membrane potential of the t-system, so that no voltage-activated Ca^{2+} fluxes interfere with the tracking of store-dependent Ca^{2+} fluxes across the t-system in these experiments.

The submaximal activation of SOCE in 0.4 mM $[Mg^{2+}]_{cyto}$ provided a means to determine whether IA65 accelerated the rate of Ca^{2+} entry through Orai1. The application of 0.4 mM $[Mg^{2+}]_{cyto}$, no added Ca^{2+}, and 10 μM IA65 to the fiber with an initial $[Ca^{2+}]_{t\text{-}sys}$ close to 1 mM caused a more rapid decline than in the same solution in the absence of IA65. Figure 6E shows the steady-state nadirs achieved in RyR-activating solutions that trigger SOCE. Maximal SOCE in caffeine reduced $[Ca^{2+}]_{t\text{-}sys}$ to the lowest level. Figure 6F presents the rate at which the $[Ca^{2+}]_{t\text{-}sys}$ transient declined during SOCE in the presence of caffeine, 0.4 mM $[Mg^{2+}]_{t\text{-}sys}$ in the absence and presence of IA65. IA65 significantly increased the rate of Orai1 activation compared to its absence for the same degree of activation of RyR Ca^{2+} conductance.[33]

DISCUSSION

While there is continuing development of inhibitors of SOCE, with four compounds (CM2489 and CM 4620 from CalciMedica; RP2128 and RP4010 from Rhizen Pharmaceuticals) reported to have entered clinical trials for various indications,[22] there is also a rising interest in the development of stimulators. These include the mineralocorticoid desoxycorticosterone acetate,[37] the borinate MDEB,[38] and some examples of the new class of pyrtriazoles,[22] but the selectivity of these compounds is not known.

The identification of 4-((5-phenyl-4-(trifluoromethyl)-thiazol-2-yl)amino)benzoic acid (IA65) as an enhancer of SOCE, despite our original aim to identify SOCE inhibitors, supports the idea that minor structural modifications of ion channel inhibitors can produce ion channel activators. This is exemplified by the ability of different enantiomers of BAYK8644 to produce activation or inhibition of L-type voltage-gated Ca^{2+} channels.[39] More specifically, the structure−activity relationships within the set of compounds assessed in this study suggests that the carboxylic acid is essential for activation of Orai1, as is its positioning para (opposite) to the central aminothiazole unit; compounds **6**−**9**, with a meta-positioned acid, were inactive. A second requirement is that the bulky aromatic substituent is appended to the 5-position of the aminothiazole (adjacent to the sulfur), which gives the molecule a reasonably linear shape. This is consistent with the putative protein-binding site being a narrow tubular or groove-shaped one with a cationic group at one end and a lipophilic region at the other. An H-bond donor and an acceptor on opposite sides in the center of the site could also accept an H-bond from the aminothiazole NH and donate one to the thiazole ring nitrogen (Figure S9).

The ability of IA65 to enhance Orai1 but not Orai3 activity places this agent as one of the most selective agents to explore Orai1-mediated SOCE in cellular signaling processes and biological events so far developed. Pharmacological modulators of SOCE have historically lacked selectivity with pronounced effects across diverse ion channel families. This is exemplified by the actions of the SOCE inhibitors Gd^{3+}, SKF96365, and 2-APB which act on a number of Ca^{2+}-permeable ion channels.[40] Even more recently described Orai1 inhibitors such as GSK-7975A, GSK-5503A, and Synta66 also have been reported to have similar inhibitory effects on Orai3.[41] The action of these agents appears to be independent of direct effects on STIM1 binding to Orai1 or to changes in the oligomerization of STIM1. These agents have been suggested instead to act via an allosteric effect on the selectivity filter of Orai channels.[41]

The mammalian Orai ion channels Orai1, Orai2, and Orai3 consist of hexamers formed by four-transmembrane subunits that assemble around a central Ca^{2+}-permeable pore. Orai3 is believed to have evolved from Orai1;[42] Orai3 has an extended N-terminus as well as truncations in the extracellular loop between transmembrane domain 3 and 4 and the C-terminus in Orai3 relative to Orai1. Given this divergence in primary structure, it is difficult to identify likely regions contributing to the observed functional selectivity of IA65. However, given the importance of the N-terminal domain of Orai1 in channel activation and CDI, this region may be contributing to activation of Orai1 by IA65. The pronounced differential effects of IA65 on Orai1 and Orai3 may indicate that this moiety could be a scaffold to achieve Orai1 inhibitors with improved selectivity over Orai3. At the very least, IA65 defines the opportunity for selective modulation of Orai isoforms, which will be critical to future studies of SOCE and/or the development of Orai1 pharmacological modulators that have less side effects due to a lack of effects on Orai3. Our identification of differential modulation of Orai1 and Orai3 by IA65 also suggests that selective Orai3 pharmacological inhibitors might be achievable. This may be of particular significance given the identification of Orai3 associated processes are important in disease states such as in the growth of estrogen receptor positive breast cancers.[43]

The studies presented here have also demonstrated the ability of enhancement of Orai1-mediated Ca^{2+} influx to influence physiological processes. Specifically, our studies with IA65 show that enhancement of the SOCE induced by PDGF is sufficient to promote the migration but not proliferation of VSMCs, suggesting that IA65 can be used to specifically fine-tune a cellular function.

Skeletal muscle possesses a unique presentation of SOCE, where it is rapidly activated in response to increases in RyR activity.[44] In our experiments where we could track the flux of Ca^{2+} through the Orai1 channel during the increased activity of the RyR, IA65 increased the rate of Ca^{2+} flux through Orai1. An increase in Orai1 Ca^{2+} flux was observed during a submaximal activation of the RyR. Our results in skeletal muscle fibers are consistent with IA65 enhancing the conductance of Ca^{2+} through Orai1 under conditions where SOCE is already partially activated.

In addition to IA65 as an exemplar for the potential for the development of more Orai isoform selective agents, IA65 and/or future analogues with similar CDI-activating properties may be useful in defining or even controlling a variety of physiological processes important in disease. For example, Orai1 activators can be used to enhance vascular smooth muscle migration to promote wound healing or to boost T- and B-cell immune function.

Gain-of-function mutations in Orai1 cause tubular aggregate myopathy (TAM), a condition caused by excessive store-dependent Ca^{2+} influx in skeletal muscle (and can also present with a mutation in STIM1 or the SR Ca^{2+}-buffer,

https://dx.doi.org/10.1021/acsptsci.9b00081
ACS Pharmacol. Transl. Sci. 2020, 3, 135−147

calsequestrin).[19] How the enhanced activation of Orai1-dependent Ca^{2+} entry leads to the characteristic tubular aggregates and muscle weakness that define the disease phenotype still remains to be elucidated. IA65 will provide a valuable tool as an Orai1 enhancer to examine Orai1-related myopathy. IA65 will provide insights into Orai1 gain-of-function TAM by providing a means of acutely accelerating Ca^{2+} entry into healthy muscle fibers.

These studies demonstrate the ability for pharmacological agents to selectively and differentially modulate Orai channel isoforms. The development of an Orai1 activity enhancer with concurrent activation of CDI has allowed the identification of a selective role for Orai1-mediated SOCE in the promotion of PDGF-induced migration of VSMCs and the role of Orai1 in Ca^{2+} homeostasis in skeletal muscle. This new tool will allow further assessment of these and other Orai1-regulated processes in different cell types such as neurons, glial cells, and lymphocytes without the potential cytotoxic effects of sustained Orai1 activation.

MATERIALS AND METHODS

Chemicals and Synthesis of the Orai1 Enhancer 4-((5-Phenyl-4-(trifluoromethyl)thiazol-2-yl)amino)benzoic acid (IA65). Compounds **1**−**20** including IA65 used for initial testing were obtained from ChemBridge Corporation (San Diego, CA). For the synthesis of larger amounts of IA65, 3-bromo-1,1,1-trifluoro-3-phenylpropan-2-one was first prepared whereby a solution of bromine (200 mg, 1.28 mmol) in trifluoromethylbenzene (1 mL) was added dropwise to a solution of 1,1,1-trifluoro-3-phenylpropan-2-one (200 mg, 1.06 mmol) in trifluoromethylbenzene (3 mL). The solution was stirred and irradiated with a 200 W lamp for 2 h. The solution was then diluted with EtOAc, washed with cold 1% sodium disulfite and water, and dried (Na_2SO_4). Vacuum flash chromatography (petroleum ether/diethyl ether; 100:0 to 12:5) gave 3-bromo-1,1,1-trifluoro-3-phenylpropan-2-one[45] (150 mg, 54%) as an unstable wax; LR-LCMS M − 1 265/267. The product was kept at −20 °C until required. For the synthesis of 4-((5-phenyl-4-(trifluoromethyl)thiazol-2-yl)-amino)benzoic acid (IA65), a solution of 3-bromo-1,1,1-trifluoro-3-phenylpropan-2-one (125 mg, 46.8 mmol) and 4-thioureidobenzoic acid (92 mg, 46.8 mmol) in dioxane (10 mL) was heated at 70 °C for 3 days. Solvents were removed, and the residue was triturated with petroleum ether and diethyl ether to yield 4-((5-phenyl-4-(trifluoromethyl)thiazol-2-yl)-amino)benzoic acid[46] (115 mg, 68%) as a white solid; mp 272−275 °C. ^{1}H NMR [$(CD_3)_2SO$] δ 12.65 (broad s, 1H), 10.99 (s, 1H), 7.93 (d, J = 8.8 Hz, 2H), 7.69 (d, J = 8.8 Hz, 2H), 7.54−7.45 (m, 5H). HRMS: found M + 1 = 365.0568, calculated M + 1 = 365.0564. HPLC purity: 98.9%.

The identities of compounds **1**−**20** and IA65 were examined by high-resolution mass spectrometry using an Agilent 6520 Accurate-Mass Q-TOF LC/MS system operating in positive electrospray ionization mode. A 10 μL aliquot of a 10 μM solution of compound in HPLC-grade methanol was injected into the instrument using an Agilent 1290 HPLC system with column bypass and the observed masses of all compounds were within 5 ppm of the calculated values.

Cell Culture. The MDA-MB-231 cell line was obtained from The American Type Culture Collection (ATCC, Manassas, VA) and maintained in Dulbecco's modified Eagle's medium (DMEM) with high glucose (Sigma-Aldrich, St Louise, MO), supplemented with 4 mM L-glutamine and 10% fetal bovine serum (FBS). The MCF7-WT cell line was obtained from ATCC. MCF7-Orai1 KO cells were generated by the Trebak laboratory by using the CRISPR/Cas9 technique. All MCF7 cells are cultured as described for MDA-MB-231 cells.

Orai1/2/3 triple-knockout HEK293 cell line was generated by the Trebak laboratory by using CRISPR/Cas9 technique as described below. STIM1 and Orai1 stable HEK293 cells are a generous gift from Donald L. Gill (Penn State University). All HEK293 cells are maintained in DMEM with high glucose (ThermoFisher Scientific, Waltham, MA), 10% FBS, and 1% antibiotic−antimycotic.

For vascular smooth muscle cell (VSMC) culture, all experiments using rats were reviewed and approved by the Institutional Animal Care and Use Committee at Pennsylvania State University College of Medicine. Adult male rats (200−300 g) were euthanized, and thoracic aortas were dissected and placed in ice-cold physiological saline solution. Adventitial and intimal layers were microdissected from the aorta. Medial layers of the aorta were diced into small pieces and placed in an enzyme solution of type II collagenase, elastase, and soybean trypsin inhibitor (Worthington Biochemical) for 60 min at 37 °C with constant agitation. The enzyme solution was removed, and VSMCs were filtered through a 100 μm cell strainer. VSMCs were seeded onto tissue culture plates and further cultured using 45% DMEM and 45% Ham's F-12 media supplemented with 10% FBS, 1% L-glutamine, and 1% antibiotic−antimycotic at 37 °C, 5% CO_2, and 100% humidity. All VSMC experiments used cells between passages 3 and 8.

Generation of Triple-Knockout Orai Channel Isoforms in HEK293 Cells and Single-Knockout Orai1 in MCF7 Cells Using CRISPR/Cas9. Orai1 gene knockout was performed as previously described.[21] Briefly, for Orai1 gene knockout, a single Orai1-specific gRNA (5′-GTTGCTCACC-GCCTCGATGT-3′) was subcloned into the lentiCRISPR v2 vector (Addgene, Plasmid #52961) to generate insertion/deletions within the Orai1 gene. Wildtype HEK293 or wildtype MCF7 cells were transfected with the corresponding Orai1-targeting vector using nucleofection. Two days after transfection, puromycin (2 μg/mL) (Gemini Bio Products, West Sacramento, CA) was added to the medium to select for cells expressing the lentiCRISPR v2 vector. At 6 days after puromycin selection, cells were collected and seeded at a density of 1 cell/well into 96-well plates. Once colonies had formed clones were screened using the Guide-it Mutation Detection Kit (Clontech Laboratories, 631443) and genetic knockout confirmed by Sanger-sequencing as follows. The Orai1 guide RNA is targeted to make a cut in the human Orai1 coding sequence between nucleotides 635 and 636. Sanger sequencing showed that in our clone of Orai1-KO HEK293, the first allele showed a 23 nucleotide deletion from nucleotides 618 to 640. The second allele has a 16 nucleotide insertion at the cut site (nucleotide 635). Both changes result in a frameshift mutation and the formation of a premature stop codon. Total Orai1 knockout was further confirmed by Western blots. For the Orai1-KO MCF7 cells, each allele was also altered in a different manner. The first allele showed a single nucleotide deletion at position 635, while the second allele has a 65 nucleotide deletion that spans from nucleotide 583 to 647. Both deletions caused frameshift mutations and an early stop codon. Total Orai1 knockout in MCF7 cells was further confirmed by Western blots.

https://dx.doi.org/10.1021/acsptsci.9b00081
ACS Pharmacol. Transl. Sci. 2020, 3, 135−147

Table 1. Quantitative PCR Primers

primers	forward	reverse
GAPDH (real-time PCR)	5′-CCCTTCATTGACCTCAACTACA-3′	5′-ATGACAAGCTTCCCGTTCTC-3′
NONO (real-time PCR)	5′-TCCGAGGAGATACCAGTCGG-3′	5′-CCTGGGCCTCTCAACTTCGAT-3′
ORAI2 (real-time PCR)	5′-TGGCGGAAGCTCTACCTGAG-3′	5′-CGGGTACTGGTACTGCGTC-3′
ORAI3 (real-time PCR)	5′-CTGGAGAGTGACCACGAGTA-3′	5′-TGGAGACCATGAGTGCAAAG-3′

We then used these Orai1 knockout HEK293 cells to generate double Orai1/Orai2 and subsequently triple Orai1/Orai2/Orai3 knockout cells. Due to the lack of specific Orai2 and Orai3 antibodies required to document absence of protein expression, we adapted a different CRISPR/Cas9 method aimed at achieving complete genomic deletion of Orai2 and Orai3 in single-knockout Orai1 clones. This allows for the use of a complete loss of mRNA in RT-qPCR assays as reliable means of establishing gene knockout. We subcloned two Orai2 (5′-ACGACAGGGCCTGTACCGAG-3′ and 5′-CTCATGCGGGGACTCGCTGA-3′) or two Orai3 (5′-GTTCGTGCACCGCGGCTACC-3′ and 5′-CCAGAGACTGCACCGCTACG-3′) specific gRNAs flanking the entire Orai2 or Orai3 gene into two fluorescent vectors (pSpCas9(BB)-2A-GFP and pU6-(BbsI)_CBh-Cas9-T2A-mCherry: Addgene). At 24 h after transfection, single cells with high expression of GFP and mCherry were sorted into 96-well plates (FACS Aria SORP high-performance cell sorter). Cells were then maintained in complete medium until colonies began to form. Visible colonies were collected, DNA extracted, and screened using specific primers designed to resolve a wildtype or knockout PCR product. Positive clones were chosen when only the knockout band was seen with no product in the wildtype reaction. The complete list of primers can be found in Table S3.

Western Blotting. Lysates were prepared using RIPA lysis buffer (Sigma) supplemented with protease inhibitors (Thermofisher Scientific). Both 30 and 50 μg samples of protein lysate were used for experiments with HEK293 and MCF7 cells, respectively. Protein was loaded into a 4−12% Bis-Tris gel (Life Technologies) and then transferred onto a PVDF membrane (Millipore). After blocking for 1 h at room temperature with Olympus Blocking Buffer (LI-COR), membranes were incubated for 2 h at room temperature with primary antibody diluted in Olympus Blocking Buffer and 0.1% Tween. The dilutions of primary antibodies were as follows: rabbit anti-ORAI1 (Sigma) 1:1000, mouse anti-HSP70 (Santa Cruz) 1:4000, mouse anti-GAPDH (Millipore) 1:3000, and mouse anti-α-tubulin (CST) 1:2000. Following four washes with 0.1% TBST for 5 min each, membranes were placed in secondary antibody diluted in Olympus Blocking Buffer and 0.1% Tween for 1 h at room temperature. The secondary antibodies were 1:10 000 680RD conjugated anti-mouse (LI-COR) and 1:5000 800CW conjugated anti-rabbit (LI-COR). After four further washes with 0.1% TBST for 5 min each, images of blots were taken using the Odyssey Clx imaging system. Densitometry was quantified using Image-Studio Lite.

Quantitative PCR. Using RNAeasy Minikit (Qiagen) total RNA was isolated from HEK293 cells and quantified using nanodrop 2000 spectrophotometer (Thermofisher Scientific). A 1 μg sample of total RNA was transcribed into cDNA using the High Capacity cDNA Reverse Transcription Kit (Applied Biosystems). In a 96-well plate, cDNA was loaded along with SYBR Green qPCR Master Mix (Applied Biosystems) and corresponding primers (Table 1). Target mRNA expression was then collected and quantified using the QuantStudio 3 real-time PCR system (Applied Biosystems) with the PCR protocol as follows: 50 °C 2 min activation step, a 95 °C 2 min melt step, 40 cycles of 95 °C for 15 s followed by 54.3 °C for 15 s and 72 °C for 30 s. To validate primer specificity, a melt curve was generated. Target mRNA expression was quantified by comparative ΔC_t method and normalized to the housekeeping genes GAPDH and NONO. All qPCR experiments were performed in technical triplicates and biological duplicates.

$[Ca^{2+}]_{CYT}$ Assays in Breast Cancer Cells. Assessment of cytosolic free Ca^{2+} ($[Ca^{2+}]_{CYT}$) was performed using a Fluorometric Imaging Plate Reader (FLIPR^{TETRA}, Molecular Devices) and PBX no-wash Ca^{2+} Assay Kit (640175, BD Biosciences) in 96- or 384-well (in the case of analogue compound analyses) black plates. At 2 days postseeding, Ca^{2+} assessment during SOCE was performed as described previously.[24] Cells were treated with IA65 at different concentrations for 15 min prior to SOCE measurement. Concentrations of IA65 were maintained during SOCE assessment. Data were analyzed using ScreenWorks Software (v2.0.0.27, Molecular Devices). Response over baseline was used as a relative measure of $[Ca^{2+}]_{CYT}$. Original IA65 and its analogues were purchased from Chembridge Corporation (San Diego, CA). For subsequent studies, IA65 was synthesized (as described above: "Chemicals and Synthesis of the Orai1 Enhancer 4-((5-Phenyl-4-(trifluoromethyl)thiazol-2-yl)-amino)benzoic acid (IA65)") and was reconfirmed for its activity.

Patch Clamp Electrophysiology. Cells were seeded onto 30 mm glass coverslips in the 6-well plates 24 h before recordings. Whole-cell patch clamp electrophysiological recordings were carried out using an Axopatch 200B and Digidata 1440A (Molecular Devices, San Jose, CA). Pipettes were pulled from borosilicate glass capillaries (World Precision Instruments) with a P-1000 Flaming/Brown micropipette puller (Sutter Instrument Company, Novato, CA) and polished using DMF1000 (World Precision Instruments, Sarasota, FL). Resistances of filled pipettes were 2−4 MΩ. Under whole-cell configuration, only cells with series resistances less than 8 MΩ and tight seals (>16 gigohms) were chosen to perform recordings. $MgCl_2$ (8 mM) was included in the pipet solution to inhibit TRPM7 currents. Clampfit 10.3 software (Molecular Devices, San Jose, CA) was used for data analysis.

For CRAC Current Recordings. We used Orai1/2/3 triple-knockout HEK293 cells transfected with 4.0 μg of a plasmid encoding eYFP-STIM1 and 1.0 μg of a plasmid encoding either CFP-Orai1 or CFP-Orai3. In some CRAC recording experiments, we used HEK293 cells stably expressing eYFP-STIM1 and CFP-Orai1. Immediately after break-in, cells were maintained at a +30 mV holding potential during experiments

https://dx.doi.org/10.1021/acsptsci.9b00081
ACS Pharmacol. Transl. Sci. 2020, 3, 135−147

and subjected to a 250 ms voltage ramps from +100 to −140 mV every 2 s until CRAC currents reached steady-state level. Bath solution: 115 mM Na-methanesulfonate, 10 mM CsCl, 1.2 mM $MgSO_4$, 10 mM Hepes, 20 mM $CaCl_2$, and 10 mM glucose (pH 7.4 with NaOH). Two different pipet solutions, containing either BAPTA or EGTA as buffer, were used and showed comparable results: Pipette solution 1: 135 mM Cs-methanesulfonate, 10 mM EGTA, 8 mM $MgCl_2$, and 10 mM Hepes (pH 7.2 with CsOH). Pipette solution 2: 115 mM Cs-methanesulfonate, 20 mM Cs-BAPTA, 8 mM $MgCl_2$, and 10 mM Hepes (pH adjusted to 7.2 with CsOH).

For CDI Data Collection. We used Orai1/2/3 triple-knockout HEK293 cells transfected with 4.0 μg of a plasmid encoding eYFP-STIM1 and 1.0 μg of a plasmid encoding either CFP-Orai1, or CFP-Orai3. Immediately after break-in and before CRAC currents have developed, we ran a stimulus protocol consisting of families of 150 ms voltage steps (from +30 mV holding potential to −120, −100, −80, and −60 mV). A 2 s interval was applied between steps. At the beginning of each pulse, a 2.5 ms voltage step to 0 mV was used to eliminate residual capacitive artifacts from cell capacitance. This first voltage step recording was used for leak subtraction. Next, a 250 ms voltage ramp from +100 to −140 mV was administered every 2 s until CRAC currents reached steady-state level (usually within 150−300 s). Once steady-state CRAC current activation was achieved, CDI was determined by performing a second round of voltage steps, using the same protocol used during the first round described above. CDI was quantified as the remaining current measured at 146 ms from the peak current at the beginning of the pulse. Bath solution: 115 mM Na-methanesulfonate, 10 mM CsCl, 1.2 mM $MgSO_4$, 10 mM Hepes, 20 mM $CaCl_2$, and 10 mM glucose (pH 7.4 with NaOH). Pipette solution: 135 mM Cs-methanesulfonate, 10 mM EGTA, 8 mM $MgCl_2$, and 10 mM Hepes (pH 7.2 with CsOH).

VSMC Proliferation and Migration Assays. VSMC proliferation was measured using the CyQUANT Cell Proliferation Assay (ThermoFisher Scientific, Waltham, MA). VSMCs were initially trypsinized, washed in PBS, and resuspended in 0.4% FBS culture media. Within the 0.4% FBS culture media, VSMCs were treated with recombinant rat PDGF-BB (R&D Systems, Minneapolis, MN) at a submaximal concentration of 0.5 ng/mL or a maximal concentration of 10 ng/mL, along with 3 or 0.5 μM IA65 or vehicle control. VSMCs were seeded at 3000 cells/well in a 96-well plate. In order to measure initial seeding density, VSMCs were allowed to attach for 3 h, and three wells from each condition were washed with PBS and stained with the CyQUANT dye for 1 h at 37 °C, 5% CO_2, and 100% humidity. Fluorescence at 485 nm excitation and 530 nm emission was then measured using a plate reader (Flexstation 3). Background fluorescence was subtracted from each well. VSMCs were then returned to 37 °C, 5% CO_2, and 100% humidity, and subsequent readings were taken at 24, 48, and 72 h. Each fluorescent reading was normalized to reading at 0 h and reported as RFU/RFU0.

To measure VSMC migration, 30 000 cells were seeded into silicon inserts with a 500 μm gap in a 6-well plate in culture media. After a monolayer of cells is formed in 24 h, culture media is removed and replaced with 0.4% FBS culture media to synchronize cells for an additional 24 h. Silicon inserts were then removed, and VSMCs were washed with PBS. VSMCs were then treated with 0.5 or 10 ng/mL recombinant rat PDGF-BB (R&D Systems, Minneapolis, MN) along with 0.5 μM IA65 or vehicle control within 0.4% FBS culture media supplemented with 10 μg/mL mitomycin C to inhibit proliferation (Sigma-Aldrich, St. Louis, MO). Bright-field images of the gap between the VSMC monolayers were taken at 0 and 12 h. Percent of gap closure was measured from subtracting the difference in gap area between 0 and 12 h using ImageJ and then normalizing this difference to the area at 0 h.

Muscle Preparation for Single Fiber Imaging. In this study we used mechanically skinned fibers to assess the influence of IA65 on t-system Ca^{2+} handling in muscle fibers.[33] This procedure involves physically peeling off the outer plasma membrane (sarcolemma) of the muscle fiber, which leaves the t-system, the invagination of the plasma membrane inside the fiber. Bathing the mechanically skinned fiber in the solution that mimics the normal cytoplasmic environment causes the t-system to re-establish a normal membrane potential. Additionally, the contractile proteins and membranes remain fully functional in regards to each of the steps in excitation−contraction coupling and SOCE.[34,47,48]

All experimental methods using rodents were approved by the Animal Ethics Committees at The University of Queensland. Male Wistar rat (6−9 weeks old) were killed by asphyxiation via CO_2 exposure, and the extensor digitorum longus (EDL) muscles were rapidly excised. Muscles were then placed in a Petri dish under paraffin oil above a layer of Sylgard. Rhod-5N salt was trapped in the sealed t-system as originally described by Lamb et al.[49] Briefly, small bundles of fibers from EDL muscles were isolated using fine forceps and exposed to a Na^+-based physiological solution (external solution) containing the following: Rhod 5N 2.5 mM; $CaCl_2$, 2.5 mM; NaCl, 132 mM; $MgCl_2$, 1 mM; KCl, 3.3 mM; Hepes, 20 mM. The pH was adjusted to 7.4 with NaOH. The dye was allowed to diffuse for 10 min or more into the t-system from the surrounding bubble of solution containing fluorescent dye. After this equilibration period, individual fibers that had been exposed to the dye solution were isolated from the bundle and mechanically skinned. After skinning, fibers were transferred to an experimental chamber containing a K^+-based internal solution which allowed the sealed t-system to generate a normal resting membrane potential.[50,51] The solution contained Mg^{2+}, 1 mM; CaEGTA/EGTA, 50; Hepes, 10 mM; K^+, 103−106 mM; Na^+, 36 mM; ATP, 8 mM; creatine phosphate, 10 mM; and *N*-benzyl-*p*-toluenesulfonamide (BTS), 0.05 mM with pH adjusted (with KOH) to 7.1. Osmolality was adjust to 290 ± 10 mOsm/kg with sucrose. Free $[Ca^{2+}]$ was set to 0 or 200 nM in this solution. To release SR Ca^{2+}, a similar solution with 30 mM caffeine, $[Mg^{2+}]$ lowered to 0.01 mM, and no added Ca^{2+} was applied to the skinned fibers.[34] To make the RyRs leaky without triggering a release of Ca^{2+} from the SR, $[Mg^{2+}]_{cyto}$ was lowered to 0.4 mM.[33]

Confocal Imaging. Mounted skinned fibers were imaged using an Olympus FV1000 confocal microscope equipped with an Olympus 0.9NA 40× Plan-Apochromat objective. Rhod-5N was excited with a 543 nm HeNe laser, and the emission was filtered using the Olympus spectra detector. For tracking Ca^{2+} movements across the t-system membrane, images were continuously recorded in *xyt* mode with an aspect ratio of 256 × 512, with the long aspect of the image parallel with that of the preparation. Temporal resolution of imaging in this mode where the fluorescence signal from within the borders of the fiber was 0.8 s.

https://dx.doi.org/10.1021/acsptsci.9b00081
ACS Pharmacol. Transl. Sci. 2020, 3, 135−147

Image Analysis for Ca^{2+} Measurements. The fluorescence of t-system rhod-5N [(t) $(F(t)$] was collected during continuous *xyt* imaging during multiple internal solution changes. At the end of the experiment, each fiber was exposed to ionophore and 5 mM Ca^{2+}, followed by 0 Ca^{2+} to obtain the fluorescence maximum (F_{max}) and minimum (F_{min}), respectively. These values were used in conjunction with the previously determined K_D of rhod-5N in the t-system of 0.8 mM[34] to determine $[Ca^{2+}]_{t\text{-}sys}$, with the relationship: $[Ca^{2+}]_{t\text{-}sys}(t) = K_{D,Ca} \times (F(t) - F_{min})/(F_{max} - F(t))$.

Selectivity Screen. A selectivity screen was conducted to assess the activity of IA65 against TRPV1, TRPM8, and $Ca_V2.2$. TRPV1 and TRPM8 assessments were performed in HEK293 cells overexpressing TRPV1 or TRPM8, and $Ca_V2.2$ assessment was conducted in SH-SY5Y neuroblastoma cells in the presence of nifedipine (10 μM), as previously described.[24] FLIPR^{TETRA} and ScreenWorks 3.2 software were used for acquiring and analyzing data.

Statistical Analysis. Data were statistically analyzed using GraphPad Prism Software (La Jolla, CA). Specific statistical tests used for each experiment are described in figure captions. A *p*-value of less than 0.05 is considered statistically significant.

■ ASSOCIATED CONTENT

Supporting Information

The Supporting Information is available free of charge at https://pubs.acs.org/doi/10.1021/acsptsci.9b00081.

> Assessment of IA65 analogues on SOCE; IA65 is not active on TRPV1, TRPM8, or CaV2.2 at concentrations up to 100 μM; oligonucleotide sequences used for RT-qPCR and cloning; IA65 did not cause cytotoxicity at concentrations that promoted SOCE; Orai1 knockout in MCF7 cells was documented by Western blot; IA65 enhanced Orai1-mediated CRAC current (I_{CRAC}); evaluation of IA65 on Orai3-mediated I_{CRAC}; Orai1 knockout in HEK293 cells; representative currents recorded from Orai1/2/3 triple-knockout HEK293 cells coexpressing STIM1 and Orai1; some possible interactions of IA65 in its putative binding pocket; uncropped full images of Figures S2 and S5 (PDF)

■ AUTHOR INFORMATION

Corresponding Authors

Mohamed Trebak − *Department of Cellular and Molecular Physiology, and Pennsylvania State Cancer Institute, The Pennsylvania State University College of Medicine, Hershey, Pennsylvania 17033, United States*; Email: mtrebak@psu.edu

Gregory R. Monteith − *School of Pharmacy and Mater Research Institute, Translational Research Institute, The University of Queensland, Brisbane 4072, Australia*; Email: greg@pharmacy.uq.edu.au

Authors

Iman Azimi − *Division of Pharmacy, College of Health and Medicine, University of Tasmania, Hobart 7001, Australia*; orcid.org/0000-0001-9477-9999

Ralph J. Stevenson − *Auckland Cancer Society Research Centre, School of Medical Sciences, The University of Auckland, Auckland 1142, New Zealand*

Xuexin Zhang − *Department of Cellular and Molecular Physiology, and Pennsylvania State Cancer Institute, The Pennsylvania State University College of Medicine, Hershey, Pennsylvania 17033, United States*

Aldo Meizoso-Huesca − *School of Biomedical Sciences, The University of Queensland, Brisbane 4072, Australia*

Ping Xin − *Department of Cellular and Molecular Physiology, and Pennsylvania State Cancer Institute, The Pennsylvania State University College of Medicine, Hershey, Pennsylvania 17033, United States*

Martin Johnson − *Department of Cellular and Molecular Physiology, and Pennsylvania State Cancer Institute, The Pennsylvania State University College of Medicine, Hershey, Pennsylvania 17033, United States*

Jack U. Flanagan − *Auckland Cancer Society Research Centre, School of Medical Sciences, The University of Auckland, Auckland 1142, New Zealand*

Silke B. Chalmers − *School of Pharmacy, The University of Queensland, Brisbane 4072, Australia*

Ryan E. Yoast − *Department of Cellular and Molecular Physiology, and Pennsylvania State Cancer Institute, The Pennsylvania State University College of Medicine, Hershey, Pennsylvania 17033, United States*

Jeevak S. Kapure − *School of Pharmacy, The University of Queensland, Brisbane 4072, Australia*

Benjamin P. Ross − *School of Pharmacy, The University of Queensland, Brisbane 4072, Australia*; orcid.org/0000-0002-1899-8484

Irina Vetter − *School of Pharmacy, The University of Queensland, Brisbane 4072, Australia; IMB Centre for Pain Research, Institute for Molecular Bioscience, University of Queensland, Brisbane 4072, Australia*

Mark R. Ashton − *UniQuest Pty Ltd, The University of Queensland, Brisbane 4072, Australia*

Bradley S. Launikonis − *School of Biomedical Sciences, The University of Queensland, Brisbane 4072, Australia*

William A. Denny − *Auckland Cancer Society Research Centre, School of Medical Sciences, The University of Auckland, Auckland 1142, New Zealand*; orcid.org/0000-0001-7997-1843

Complete contact information is available at: https://pubs.acs.org/10.1021/acsptsci.9b00081

Author Contributions

●G.R.M. and M.T. are joint corresponding authors. I.A., R.J.S., X.Z., A.M.-H., M.J., S.B.C., P.X., and R.E.Y. conducted and analyzed the biological experiments. J.S.K. and B.P.R. confirmed the identities of compounds **1**−**20** and IA65 by high-resolution mass spectrometry. I.V. led the completion of the selectivity testing. W.A.D. and J.U.F. designed the chemical library for Orai1 activity assessment that led to the identification of IA65 as a Orai1 modulator. R.J.S. and W.A.D. designed the synthesis of IA65 and R.J.S. carried out the synthesis of IA65. M.R.A. selected IA65 analogues for further testing on Orai1 activity. I.A., B.S.L., M.T., and G.R.M. designed the biological experiments and supervised studies. All authors contributed to the writing of the manuscript.

Notes

The authors declare the following competing financial interest(s): G.R.M. and W.A.D. are associated with QUE Oncology Inc.

https://dx.doi.org/10.1021/acsptsci.9b00081
ACS Pharmacol. Transl. Sci. 2020, 3, 135−147

■ ACKNOWLEDGMENTS

We gratefully acknowledge funding from QUE Oncology Inc. and the University of Auckland Biopharma Initiative. We acknowledge reagents and fruitful discussions with Don Gill and members of his laboratory. Research in the Trebak laboratory is supported by grants R01HL123364 and R01HL097111 from the National Institutes of Health to M.T. This work was supported by an Australian Research Council Discovery Project to B.S.L. and G.R.M. (DP180100937). G.R.M. was supported by the Mater Foundation. The Translational Research Institute is supported by a grant from the Australian Government.

■ REFERENCES

(1) Berridge, M. J., Bootman, M. D., and Roderick, H. L. (2003) Calcium signalling: dynamics, homeostasis and remodelling. *Nat. Rev. Mol. Cell Biol. 4*, 517−529.

(2) Gudlur, A., and Hogan, P. G. (2017) The STIM-Orai Pathway: Orai, the Pore-Forming Subunit of the CRAC Channel. *Adv. Exp. Med. Biol. 993*, 39−57.

(3) Cai, X., et al. (2016) The Orai1 Store-operated Calcium Channel Functions as a Hexamer. *J. Biol. Chem. 291*, 25764−25775.

(4) Hou, X., Pedi, L., Diver, M. M., and Long, S. B. (2012) Crystal structure of the calcium release-activated calcium channel Orai. *Science 338*, 1308−1313.

(5) Feske, S., et al. (2006) A mutation in Orai1 causes immune deficiency by abrogating CRAC channel function. *Nature 441*, 179−185.

(6) Roos, J., et al. (2005) STIM1, an essential and conserved component of store-operated Ca2+ channel function. *J. Cell Biol. 169*, 435−445.

(7) Smyth, J. T., et al. (2006) Emerging perspectives in store-operated Ca2+ entry: roles of Orai, Stim and TRP. *Biochim. Biophys. Acta, Mol. Cell Res. 1763*, 1147−1160.

(8) Lacruz, R. S., and Feske, S. (2015) Diseases caused by mutations in ORAI1 and STIM1. *Ann. N. Y. Acad. Sci. 1356*, 45−79.

(9) McCarl, C. A., et al. (2010) Store-operated Ca2+ entry through ORAI1 is critical for T cell-mediated autoimmunity and allograft rejection. *J. Immunol. 185*, 5845−5858.

(10) Davis, F. M., et al. (2015) Essential role of Orai1 store-operated calcium channels in lactation. *Proc. Natl. Acad. Sci. U. S. A. 112*, 5827−5832.

(11) Kar, P., and Parekh, A. B. (2015) Distinct spatial Ca2+ signatures selectively activate different NFAT transcription factor isoforms. *Mol. Cell 58*, 232−243.

(12) Stauderman, K. A. (2018) CRAC channels as targets for drug discovery and development. *Cell Calcium 74*, 147−159.

(13) Tian, C., Du, L., Zhou, Y., and Li, M. (2016) Store-operated CRAC channel inhibitors: opportunities and challenges. *Future Med. Chem. 8*, 817−832.

(14) Wen, L., Voronina, S., Javed, M. A., Awais, M., Szatmary, P., Latawiec, D., Chvanov, M., Collier, D., Huang, W., Barrett, J., et al. (2015) Inhibitors of ORAI1 Prevent Cytosolic Calcium-Associated Injury of Human Pancreatic Acinar Cells and Acute Pancreatitis in 3 Mouse Models. *Gastroenterology 149*, 481−492.

(15) Yang, S., Zhang, J. J., and Huang, X. Y. (2009) Orai1 and STIM1 are critical for breast tumor cell migration and metastasis. *Cancer Cell 15*, 124−134.

(16) Zhang, S. L., et al. (2008) Store-dependent and -independent modes regulating Ca2+ release-activated Ca2+ channel activity of human Orai1 and Orai3. *J. Biol. Chem. 283*, 17662−17671.

(17) Bogeski, I., Al-Ansary, D., Qu, B., Niemeyer, B. A., Hoth, M., and Peinelt, C. (2010) Pharmacology of ORAI channels as a tool to understand their physiological functions. *Expert Rev. Clin. Pharmacol. 3*, 291−303.

(18) Motiani, R. K., Abdullaev, I. F., and Trebak, M. (2010) A novel native store-operated calcium channel encoded by Orai3: selective requirement of Orai3 versus Orai1 in estrogen receptor-positive versus estrogen receptor-negative breast cancer cells. *J. Biol. Chem. 285*, 19173−19183.

(19) Bohm, J., and Laporte, J. (2018) Gain-of-function mutations in STIM1 and ORAI1 causing tubular aggregate myopathy and Stormorken syndrome. *Cell Calcium 76*, 1−9.

(20) Mullins, F. M., Park, C. Y., Dolmetsch, R. E., and Lewis, R. S. (2009) STIM1 and calmodulin interact with Orai1 to induce Ca2+-dependent inactivation of CRAC channels. *Proc. Natl. Acad. Sci. U. S. A. 106*, 15495−15500.

(21) Zhang, X., Pathak, T., Yoast, R., Emrich, S., Xin, P., Nwokonko, R. M., Johnson, M., Wu, S., Delierneux, C., Gueguinou, M., et al. (2019) A calcium/cAMP signaling loop at the ORAI1 mouth drives channel inactivation to shape NFAT induction. *Nat. Commun. 10*, 1971.

(22) Riva, B., et al. (2018) Pyrtriazoles, a Novel Class of Store-Operated Calcium Entry Modulators: Discovery, Biological Profiling, and in Vivo Proof-of-Concept Efficacy in Acute Pancreatitis. *J. Med. Chem. 61*, 9756−9783.

(23) McAndrew, D., et al. (2011) ORAI1-mediated calcium influx in lactation and in breast cancer. *Mol. Cancer Ther. 10*, 448−460.

(24) Azimi, I., et al. (2017) Evaluation of known and novel inhibitors of Orai1-mediated store operated Ca(2+) entry in MDA-MB-231 breast cancer cells using a Fluorescence Imaging Plate Reader assay. *Bioorg. Med. Chem. 25*, 440−449.

(25) Sadaghiani, A. M., et al. (2014) Identification of Orai1 channel inhibitors by using minimal functional domains to screen small molecule microarrays. *Chem. Biol. 21*, 1278−1292.

(26) Stevenson, R. J., et al. (2018) An SAR study of hydroxy-trifluoromethylpyrazolines as inhibitors of Orai1-mediated store operated Ca(2+) entry in MDA-MB-231 breast cancer cells using a convenient Fluorescence Imaging Plate Reader assay. *Bioorg. Med. Chem. 26*, 3406−3413.

(27) Chantome, A., et al. (2013) Pivotal role of the lipid Raft SK3-Orai1 complex in human cancer cell migration and bone metastases. *Cancer Res. 73*, 4852−4861.

(28) Didiasova, M., et al. (2015) STIM1/ORAI1-mediated Ca2+ Influx Regulates Enolase-1 Exteriorization. *J. Biol. Chem. 290*, 11983−11999.

(29) Vandenberghe, M., et al. (2013) ORAI1 calcium channel orchestrates skin homeostasis. *Proc. Natl. Acad. Sci. U. S. A. 110*, E4839−4848.

(30) Potier, M., et al. (2009) Evidence for STIM1- and Orai1-dependent store-operated calcium influx through ICRAC in vascular smooth muscle cells: role in proliferation and migration. *FASEB J. 23*, 2425−2437.

(31) Zhang, W., et al. (2011) Orai1-mediated I (CRAC) is essential for neointima formation after vascular injury. *Circ. Res. 109*, 534−542.

(32) Launikonis, B. S., Barnes, M., and Stephenson, D. G. (2003) Identification of the coupling between skeletal muscle store-operated Ca2+ entry and the inositol trisphosphate receptor. *Proc. Natl. Acad. Sci. U. S. A. 100*, 2941−2944.

(33) Cully, T. R., Choi, R. H., Bjorksten, A. R., Stephenson, D. G., Murphy, R. M., and Launikonis, B. S. (2018) Junctional membrane Ca(2+) dynamics in human muscle fibers are altered by malignant hyperthermia causative RyR mutation. *Proc. Natl. Acad. Sci. U. S. A. 115*, 8215−8220.

(34) Cully, T. R., Edwards, J. N., Murphy, R. M., and Launikonis, B. S. (2016) A quantitative description of tubular system Ca(2+) handling in fast- and slow-twitch muscle fibres. *J. Physiol. 594*, 2795−2810.

(35) Cully, T. R., Murphy, R. M., Roberts, L., Raastad, T., Fassett, R. G., Coombes, J. S., Jayasinghe, I. D., Launikonis, B. S., et al. (2017) Human skeletal muscle plasmalemma alters its structure to change its Ca(2+)-handling following heavy-load resistance exercise. *Nat. Commun. 8*, 14266.

(36) Cummings, M. C., Chambers, R., Simpson, P. T., and Lakhani, S. R. (2011) Molecular classification of breast cancer: is it time to pack up our microscopes? *Pathology 43*, 1−8.

https://dx.doi.org/10.1021/acsptsci.9b00081
ACS Pharmacol. Transl. Sci. 2020, 3, 135−147

(37) Liu, G., et al. (2013) Upregulation of store operated Ca channel Orai1, stimulation of Ca(2+) entry and triggering of cell membrane scrambling in platelets by mineralocorticoid DOCA. *Kidney Blood Pressure Res. 38*, 21−30.
(38) Djillani, A., et al. (2015) Potentiation of the store-operated calcium entry (SOCE) induces phytohemagglutinin-activated Jurkat T cell apoptosis. *Cell Calcium 58*, 171−185.
(39) Franckowiak, G., Bechem, M., Schramm, M., and Thomas, G. (1985) The optical isomers of the 1,4-dihydropyridine BAY K 8644 show opposite effects on Ca channels. *Eur. J. Pharmacol. 114*, 223−226.
(40) Bird, G. S., Putney, J. W., Kozak, J. A., and Putney, J. W. (2017) Pharmacology of Store-Operated Calcium Entry Channels. *Calcium Entry Channels in Non-Excitable Cells*, 311.
(41) Derler, I., et al. (2013) The action of selective CRAC channel blockers is affected by the Orai pore geometry. *Cell Calcium 53*, 139−151.
(42) Shuttleworth, T. J. (2012) Orai3–the 'exceptional' Orai? *J. Physiol. 590*, 241−257.
(43) Motiani, R. K., et al. (2013) Orai3 is an estrogen receptor alpha-regulated Ca(2)(+) channel that promotes tumorigenesis. *FASEB J. 27*, 63−75.
(44) Launikonis, B. S., and Rios, E. (2007) Store-operated Ca2+ entry during intracellular Ca2+ release in mammalian skeletal muscle. *J. Physiol. 583*, 81−97.
(45) Pinder, R. M., and Burger, A. (1967) Trifluoromethyl analogs of amphetamine and norephedrine. *J. Pharm. Sci. 56*, 970−973.
(46) Karavan, V. S., and Nikiforov, V. A. (1999) Formation of Thiazoles by Reaction of 2-Alkoxy-2-trifluoromethyl-3-phenyloxiranes with Thioureas. *Russ. J. Org. Chem. 35*, 741−745.
(47) Edwards, J. N., Cully, T. R., Shannon, T. R., Stephenson, D. G., and Launikonis, B. S. (2012) Longitudinal and transversal propagation of excitation along the tubular system of rat fast-twitch muscle fibres studied by high speed confocal microscopy. *J. Physiol. 590*, 475−492.
(48) Lamb, G. D., and Stephenson, D. G. (2018) Measurement of force and calcium release using mechanically skinned fibers from mammalian skeletal muscle. *J. Appl. Physiol. 125*, 1105−1127.
(49) Lamb, G. D., Junankar, P. R., and Stephenson, D. G. (1995) Raised intracellular [Ca2+] abolishes excitation-contraction coupling in skeletal muscle fibres of rat and toad. *J. Physiol. 489*, 349−362.
(50) Lamb, G. D., and Stephenson, D. G. (1990) Calcium release in skinned muscle fibres of the toad by transverse tubule depolarization or by direct stimulation. *J. Physiol. 423*, 495−517.
(51) Lamb, G. D., and Stephenson, D. G. (1994) Effects of intracellular pH and [Mg2+] on excitation-contraction coupling in skeletal muscle fibres of the rat. *J. Physiol. 478*, 331−339.

https://dx.doi.org/10.1021/acsptsci.9b00081
ACS Pharmacol. Transl. Sci. 2020, 3, 135−147